Science of the Total Environment 752 (2021) 142164

Contents lists available at ScienceDirect

Science of the Total Environment

journal homepage: www.elsevier.com/locate/scitotenv

Redistribution of iron oxides in aggregates induced by pe + pH variation alters Cd availability in paddy soils

Shanshan Li, Shibao Chen *, Meng Wang, Xiaoqin Lei, Han Zheng, Xiaoyi Sun, Lifu Wang, Yun Han

Key Laboratory of Plant Nutrition and Fertilizer, Agriculture and Rural Affairs, Institute of Agricultural Resources and Regional Planning, Chinese Academy of Agricultural Sciences, Beijing 100081, PR China

HIGHLIGHTS

- Low pe + pH condition induces the decline in level of crystallinity of Fe oxides.
- Low-crystalline Fe oxides exhibit high adsorption affinity of Cd in paddy soil.
- Soil pe + pH decline favours the accumulation of Fe_o and Fe_p in larger aggregates.
- Fe redistribution in different-sized aggregates affects Cd availability in soil.

GRAPHICAL ABSTRACT

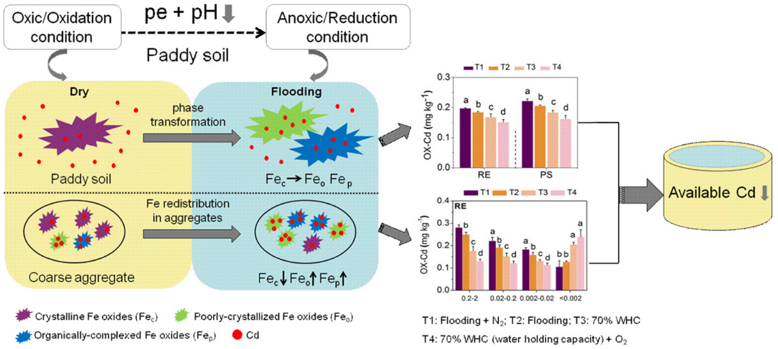

ARTICLE INFO

Article history:
Received 4 July 2020
Received in revised form 11 August 2020
Accepted 1 September 2020
Available online 2 September 2020

Editor: Xinbin Feng

Keywords:
pe + pH
Cd availability
Fe oxides
Aggregate
Paddy soil

ABSTRACT

In this study, the effect of unstable pe + pH levels on the transformation of Fe oxides in different-sized soil fractions and its impact on Cd speciation were explored. Paddy soil samples collected from two locations in China were cultivated for two months under one of four pe + pH conditions: flooding + N_2 (T1), flooding (T2), 70% water holding capacity (T3), and 70% water holding capacity + O_2 (T4). Chemical analysis and X-ray diffraction (XRD) were used to identify the mineralogical phases and species of Fe and Cd in paddy soils. The results show that the decrease of soil pe + pH level favored the transformation of well-crystallized Fe oxides (Fe_c), such as hematite and goethite, into poorly-crystallized (Fe_o) and organically-complexed (Fe_p) forms. The transformation promoted the binding of Cd to Fe oxides and was primarily responsible for up to a 41.8% decrease of soil DTPA (diethylenetriaminepentaacetic acid)-extractable-Cd content. In addition, the decline in pe + pH value reduced Fe concentrations in soil particle fractions of 0.2–2-mm (17.8%–30.6%) and <0.002-mm (20.7%–31.7%) of the two flooding treatments. The decreased Fe concentrations were closely associated with less Fe_c contents in these same fractions and more Fe_o and Fe_p in coarser aggregates ($P < 0.01$). Importantly, the increase in contents of Fe_o and Fe_p in the 0.002–2 mm fraction were significantly correlated with content of Fe-/Mn-oxide-bound Cd (OX-Cd) in larger particle-size fractions ($P < 0.01$). Furthermore, the increasing content of OX-Cd played a crucial role in reducing DTPA-Cd content. This study demonstrates that low pe + pH values favor the transformation of crystalline Fe oxides into a poorly-crystallized and organically-complexed phase, which facilitates Cd accumulation in coarser aggregates and enhances Cd stability in paddy soils.

---

* Corresponding author at: No. 12 Zhongguancun South Street, Beijing 100081, PR China.
E-mail address: chenshibao@caas.cn (S. Chen).

https://doi.org/10.1016/j.scitotenv.2020.142164
0048-9697/

1. Introduction

Iron oxides are one of the most bountiful and active metallic oxides in soils. They provide an abundance of adsorption sites for pollutants, which is important to the environmental behavior and fate of heavy metal cadmium in soils (Zhang et al., 2014). In paddy soils, periodic variations in Eh and pH levels occur in association with irrigation practices of alternating wet and dry periods in soils during the cultivation of rice (Yu et al., 2016). Moreover, the changes of levels of O_2 released from roots of rice at different growth stages also affect Eh and pH (Yu et al., 2016). The changes of pH and Eh in paddy soil may result in the transformation of iron oxides due to their high redox sensitivity, and consequently affect Cd adsorption capacity of iron oxides (Ji et al., 2019). For example, the reduction and dissolution of Cd-bearing ferric oxides at low Eh level (referred to as reducing conditions) can lead to Cd release (Fan et al., 2014). In contrast, ferrous oxides are readily oxidized to ferric oxides at circumneutral pH, and subsequently may form secondary iron minerals that can adsorb or co-precipitate with Cd (Borch et al., 2010; Muehe et al., 2013). Under acidic conditions, the reaction between proton and hydroxyl groups (-OH) or O on iron mineral surfaces increases Fe solubility and Cd availability in soil (Wu et al., 2019).

There is a close relationship between soil pH and Eh. Reportedly, soil Eh decreases under reducing conditions due to microbial consumption of O_2 (Sun et al., 2007). Meanwhile, the consumption of protons during reduction causes the rise of soil pH (Sun et al., 2007). In paddy soils, the fluctuation of pH and Eh can cause the repeated reduction-dissolution or oxidation-reprecipitation of Fe oxides. The possible redox reactions are as follows (Brennan and Lindsay, 1996).

$$Fe_3O_4\ (\text{amorp}) + 8H^+ + 2e^- \rightleftharpoons Fe^{2+} + H_2O \tag{1}$$

$$Fe(OH)_3\ (\text{amorp}) + 3H^+ + e^- \rightleftharpoons Fe^{2+} + 3H_2O \tag{2}$$

From the formulas, the consumption or accumulation of electrons (e^-) and protons (H^+) occurs simultaneously in iron-redox processes. The behavior of electrons and protons can be represented by the redox parameter pe + pH (Zheng et al., 2019). According to Brennan and Lindsay (1998), the activity of Fe^{2+} is also closely related to pe + pH:

$$3\ \log Fe^{2+} = 40.65 - 2(pe + pH) - 6pH. \tag{3}$$

Therefore, the total effect of variation in Eh and pH (pe + pH) should be taken into account in studies on the transformation of iron oxides and its impact on Cd immobilization in soil. However, studies on the transformation of Fe oxides in paddy soil rarely focus on the influence of soil pe + pH conditions.

Iron oxide, as one of the soil inorganic colloids, can promote the cohesion of free primary particles and clay minerals to form micro-aggregates (<0.25 mm) (Six et al., 2004; Xue et al., 2019a). Usually, iron oxides are heterogeneously distributed in various soil particle-size fraction. Xue et al. (2019b) reported that Fe_d (free Fe oxide), Fe_o (amorphous Fe oxide) and Fe_p (organically-complexed Fe oxide) respectively dominate in sand-sized (0.053–2 mm), clay-sized (<0.053 mm) and macro-aggregate (>5 mm) fractions of soil. While Huang et al. (2016) noted that Fe_o content was higher in small macro-aggregates (0.25–2 mm) and micro-aggregates (0.053–0.25 mm) fractions than in other fractions. The content and chemical forms of iron oxides would affect the structure and stability of aggregates (Zhao et al., 2017; Krause et al., 2020). Recent studies have found that the content of Fe_d positively correlates with mass of the micro-aggregates in soil and Fe_p content was the crucial driving factor for aggregate stability (Yin et al., 2016; Xue et al., 2019a). In paddy soil, the redox transformation of Fe oxides and turnover of aggregates, due to the variation in soil water content, have great impact on Fe distribution in different fractions (Huang et al., 2018; Krause et al., 2020). As previously reported by Huang et al. (2016), the alternation of wetting-drying irrigation accelerates the precipitation of newly formed Fe_o and Fe_p, and thus increases the Fe_o content in micro-aggregates. The redistribution of Fe oxides inevitably causes the migration of Fe-associated Cd in differently-sized aggregates, and consequently affects Cd availability in paddy soils. Currently, the majority of studies focus on the effect of Fe speciation on the formation and stability of soil aggregates (Zhao et al., 2017; Xue et al., 2019a, 2019b). However, limited information is available concerning the relationship between Fe distribution in different-sized aggregates and Cd availability in paddy soil.

The aims of this study were: (1) to explore the phase transformation of Fe oxides in paddy soil under variable pe + pH conditions; (2) to detect the effect of soil pe + pH on Fe distribution in aggregates; and (3) to investigate the relationships among soil pe + pH, Fe speciation, Fe distribution in aggregates and Cd availability in paddy soil. Herein, we hypothesized that the variation in pe + pH levels in paddy soil, resulting in the transformation and redistribution of Fe oxides in aggregates, will subsequently affect Cd availability. In order to test our hypothesis, a cultivation experiment was conducted to disclose the underlying mechanisms of variable pe + pH conditions on Cd immobilization in paddy soil.

2. Materials and methods

2.1. Soil preparation

Two types of soils (upper 0–20 cm) were sampled from Xiangtan (27° 49′ N, 112° 56′ E) and Changsha (28°15′ N, 112° 59′ E) in Hunan province, which is a major rice-growing province in China. The soil was air dried and passed through a 2-mm sieve to remove roots and stones for incubation experiments. Some soil samples were finely ground to pass through a 0.15-mm sieve to obtain data on soil chemical properties. The Eh and pH of soils were measured by a pH/mV meter with a combined Pt and Ag/AgCl electrode system (Denver Instrument UB-7, ultraBASIC, Denver Instrument, U.S.A.) from a slurry of each sample (soil: water = 1:2.5 w/w) (Qiao et al., 2018). The pipette method was used to determine the soil texture and clay content (Taubner et al., 2009). The cation exchange capacity and concentration of soil organic carbon were determined using the unbuffered silver-thiourea method and potassium bichromate titrimetric method, respectively (Qiao et al., 2018). The Fe and Cd in soils were digested by aqua regia and hydrofluoric acid, and Fe/Cd concentration of the extracts were analyzed by ICP-MS (7700×, Agilent, USA). The basic physical and chemical properties of the samples of soil are shown in Table 1.

Every 1.5 kg sampled soil was placed into a PVC pot (height 16 mm, diameter 13 mm). A solution of Cd was prepared by dissolving 3.7 mg of cadmium chloride ($CdCl_2 \cdot 2.5H_2O$) in 500 mL deionized water. The solution was added to and blended thoroughly with 1.5 kg of air-dried soil to artificially create Cd-contaminated soil with a Cd concentration of 1.2 mg kg^{-1}, which was two- (0.6 mg kg^{-1} at pH = 6.5–7.5) or three-fold (0.4 mg kg^{-1} at pH = 5.5–6.5) higher than the acceptable limit of Cd in paddy soil according to national standards for soil quality

Table 1
The basic physical and chemical properties of tested soils.

Soil properties	Soil samples	
Location	XiangTan	ChangSha
pH	6.15	6.57
Soil type	Red earth (RE)	Paddy soil (PS)
Clay (%)	30.6	25.8
OM (%)	1.53	1.91
CEC (cmol kg^{-1})	15.1	19.2
Fe content (g kg^{-1})	60.2	55.8
Cd content (mg kg^{-1})	0.11	0.13

(China, GB15618-2018). All the pots were watered to 70% field capacity and maintained for two months to reach soil equilibration.

2.2. Incubation experiments

The common irrigation practice of alternating between dry and wet periods in rice fields and the variation in release of oxygen from rice roots at different growth stages contribute to the variability in pe + pH levels in paddy soils. To simulate possible scenarios of variation in soil pe + pH, the following treatments were applied to the pots to regulate soil pe + pH levels: T1) flooding and supplemental nitrogen, T2) flooding, T3) 70% field capacity, and T4) 70% field capacity and supplemental oxygen. Submergence treatments (T1 and T2) were continuously flooded with a 3–4-cm depth of standing water throughout the incubation period. The weighing method was applied to maintain the 70% water holding capacity of soils for T3 and T4. For the T1 or T4 treatments, an electric gas pump apparatus was utilized to add oxygen or nitrogen in the soil and these pots were capped to prevent evaporation and ventilation during the soil cultivation process. The cap was equipped with both inlet and outlet pipes (diameter = 10 mm); the inlet pipe was connected to the gas pump for O_2/N_2 input. The soil samples in the T4 and T1 treatments were first flushed with the respective O_2 or N_2 for 1 min before closing the valve on the exhaust pipe, and then we continued to flush each sample for 30 s. The procedure was repeated every three days until the end of the experiment. Soils of each of the two sampling sites were used for the four treatments and each treatment had three replicates. The pots were arranged randomly and placed at approximately room temperature (20–25 °C) under natural light in a greenhouse at the Chinese Academy of Agricultural Sciences in Beijing, China. The experiment lasted for 60 days.

2.3. Measurements and analysis

At the end of the experiment, in-situ measurements of pH and Eh were obtained by a portable pH and ORP meter (FJA-6, Nanjing Chuan-Di Instrument and Equipment Co. LTD, China). The pe was calculated by dividing the value of Eh (mV) by 59.2 (Hanif et al., 1986). Soil sub-samples collected from each pot were centrifugated to separate water from soil. The supernatant of soil was discarded and half of the residue was used for aggregate-size separation. Isolation of soil aggregates was based on the method proposed by Zhang et al. (2007). A probe-type ultrasonic disaggregator (Shanghai Zhixin, JVD-650), set at an output energy of 0.2 kJ g^{-1} for 5 min, was applied to disperse the soil-water suspension. The aggregate fractions of 0.2–2, 0.02–0.2, 0.002–0.02 and <0.002 mm were obtained through wet sieving, siphonage and centrifugation. The remainder of the centrifuged soil was immediately freeze-dried in order to prevent oxidation of soil and then ground to a fine powder (<0.15 mm) for further analysis.

An X-ray diffractometer (Bruker D8 Advance, Karlsruhe, Germany) was used to identify the crystalline components of Fe oxides in the potted soils of each treatment. The available Cd in bulk soil and each aggregate-size fraction were extracted by a 25-ml leach liquor (0.005 M DTPA + 0.01 M TEA + 0.01 M $CaCl_2$); the fraction of Cd bound to Fe—Mn oxides in soil samples were extracted with NH_2OH-HCl (1 M) by the modified Tessier method (Tessier et al., 1996). The total concentration of Fe and Cd in soils was analyzed by digesting with a solution of HCl-HNO_3-H_2O_2 in a microwave digestion apparatus (Milestone MLS 1200 Mega). The extractions of the Fe_d, Fe_o, and Fe_p were respectively carried out with a dithionite-citrate-bicarbonate solution, a 0.2 M NH_4^+ oxalate buffer, and a sodium pyrophosphate solution according to Xue et al. (2019b). The concentrations of total Fe, free Fe oxides, amorphous Fe oxides and organically-complexed Fe oxides in soil were indicated by Fe_t, Fe_d, Fe_o, Fe_p, respectively; and the difference between values of Fe_d and Fe_o represented the content of crystalline Fe oxides (Fe_c). After filtering, the Fe/Cd concentrations of all the extracts were analyzed by ICP-MS (7700×, Agilent, USA).

2.4. Statistical analysis

All data were analyzed using SPSS v16.0 for Windows (IBM, USA). The significant differences among various treatments were determined by one-way analysis of variance (ANOVA) at $P < 0.05$. The data of means ± standard deviations (SD) are shown in figures and tables. Pearson's correlation coefficients for the relationships among soil pe + pH, Fe species, Cd speciation were calculated in Python (PyCharm v 2020.1.2, JetBrains, CZ).

3. Results and discussion

3.1. Changes in pe + pH and Fe speciation

The pe + pH values differed greatly under different treatments (Fig. 1), ranging from 3.42 to 11.92, due to the transfer of protons (H^+) and electrons (e^-) under different redox conditions in each soil system. The values of pe + pH, as measured in continuous flooding soils (T2), were 5.43 and 5.68 for RE and PS soils, respectively. Addition of nitrogen in T1 resulted in markedly lower soil pe + pH values by about 2.01 (RE) and 1.7 (PS) units on average. Under the flooding treatments, the inherent result of oxygen depletion produced an anoxic and reduced soil condition where an abundance of redox-sensitive elements (such as Fe, S, Mn, C, N) were likely reduced, causing a dramatic drop in soil Eh (Sun et al., 2007; Wu et al., 2019). Meanwhile, H^+ consumption due to reducing reactions occurring in soil, as well as pH regulation by CO_2 (H_2CO_3-HCO_3^- reaction), were responsible for a slight rise of soil pH from mildly acidic (the original pH values of the RE soil was 6.15 and the PS soil was 6.57) to approximately neutral (Sun et al., 2007; Pan et al., 2014). Eventually, the flooding treatment resulted in low soil pe + pH, and the supplement of nitrogen to displace the ambient air exacerbated the soil oxygen deficit, which further decreased the pe + pH level of soils. Compared to values of the T1 and T2 treatments, the pe + pH values in non-flooded soils (T3 and T4 treatments) were noticeably greater in soils from both sampling locations. The greater values may be attributed to the increase in oxygen content in the pores of the paddy soil when the pots of soil were allowed to dry and/or supplemental oxygen increasing the oxidation-reduction activity in the soil.

The variation of the pe + pH value strongly modified the level of crystallinity of Fe oxides in the two paddy soils (Fig. 2). With the drop in soil pe + pH level, the amount of Fe_c significantly decreased by 8.6%–33.6%, while the content of Fe_o increased by 30.3%–119% in soils, compared to the highest pe + pH level (T4 treatment). These results suggest that the low pe + pH conditions contributed to the decrease in level of crystallinity of Fe oxides. In reduced conditions, the high redox sensitivity of Fe causes Fe(III) oxides to biologically reduce to Fe(II) (Winkler et al., 2018). In general, the dissolved Fe(II) are readily re-oxidized and hydrolyzed to form Fe(III) oxide precipitates; the newly-formed deposits are dominated by short-range ordered oxides (such as ferrihydrite) with lower crystallinity (Winkler et al., 2016, 2018). Accordingly, the decrease of soil pe + pH and increase of soil reduction facilitated the reductive dissolution of iron oxide and its subsequent re-oxidation, consequently promoting the transformation of iron oxides from a crystalline state into an amorphous (or poorly crystallized) form. Meanwhile, the 39.1%–167% increase in the amount of Fe_p in soils with the decrease of soil pe + pH levels was observed (Fig. 2). It should be noted that Fe_p represented the content of organically-complexed iron oxides, the corresponding increased amount indicates more iron oxides bound to organic matter under anaerobic conditions. This increase may be associated with the accumulation of organic matter and low-crystalline Fe oxides in the flooded soils. The decrease of aerobic microbial activity under anaerobiosis slows the rate of decomposition and mineralization of organic matter in soils, which contributes to the net accumulation of organic matter in soils (Sahrawat, 2004). The compounds, such as polycyclic

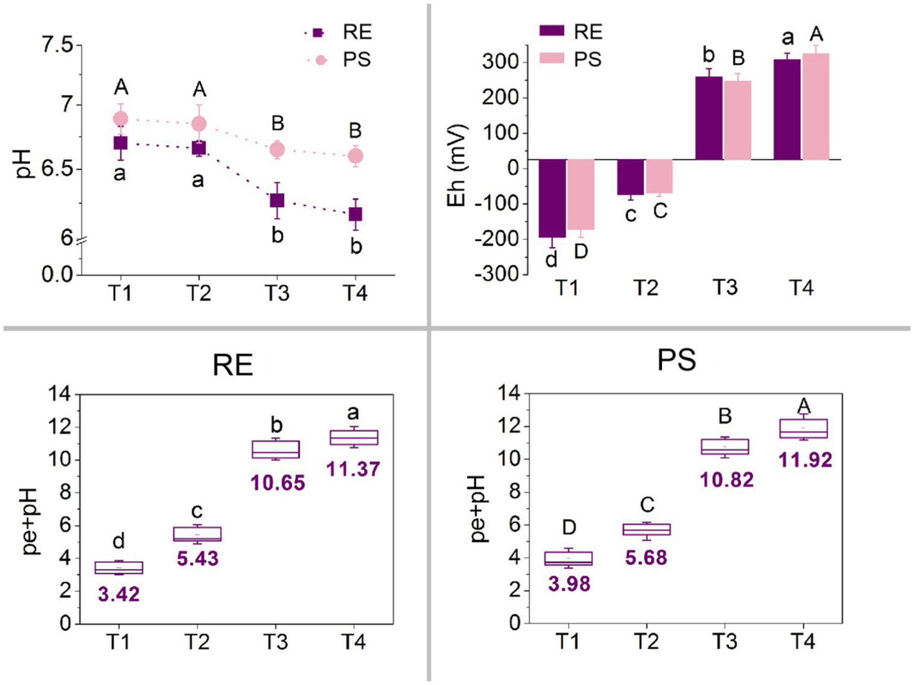

Fig. 1. Changes in pH, Eh and pe + pH levels in RE and PS soils under different treatments. The numbers represent the pe + pH values of different treatments. Different lowercase letters and capital letters respectively indicate statistically significant differences between various treatments in RE and PS soils according to *t*-tests ($P < 0.05$).

aromatics, polyphenols and carboxyls, in soil organic matter (SOM) have higher affinity for amorphous iron oxides (Wang et al., 2019). It has been ranked the adsorption capacity of iron minerals for SOM in the order of: ferrihydrite > iron sulfide > hematite > pyrite (Lv et al., 2016; Wang et al., 2019). Consequently, the ferrihydrite and iron sulfides that formed at relatively lower pe + pH levels partially adsorbed or co-precipitated with the accumulated organic matter to form organically complexed iron oxides. Notably, the sum of concentrations of crystalline and amorphous Fe oxides was slightly smaller at lower pe + pH conditions than the sum at high pe + pH conditions (Fig. 2). The difference in sums may be attributed to the reduction of iron oxides which released partial soluble Fe^{2+} into the overlying water that was discarded from the flooding treatments. Moreover, partial amorphous iron oxides complexed with organic matter also led to the decrease in the sum of contents of Fe_c and Fe_o.

The typical XRD patterns of iron oxides observed from soils under different treatments are shown in Fig. 3. We collected XRD data in the angular range of 10°–70°. The diffraction peaks representing well-crystallized goethite, hematite and magnetite were observed in both RE and PS soils, which were consistent with previous studies (Wang et al., 2009; Jiang et al., 2017). The abundances of goethite ($2\theta = 36.7°$) in RE and PS soils and hematite ($2\theta = 64.0°$) in PS soil of the T1 and T2 treatments (pe + pH below 6.0) were obviously lower than compared to abundances in the other two treatments (at pe + pH above 10.0). This suggests that goethite and hematite might be partially reduced and dissolved at low pe + pH levels; they likely transforms into amorphous forms and/or the low-crystallized phase. This result further illustrates that a low pe + pH value promotes the decrease of crystallinity of iron oxides in soils. In contrast, there were no noticeable changes in magnetite as it was more stable under either the reducing or acidic conditions (Li et al., 2019). Moreover, the weak peak of 6-line ferrihydrite ($2\theta = 53.6°$) observed in the flooded PS soils further confirmed the reductive dissolution of crystalline Fe oxides and the formation of poorly-crystallized Fe oxides at low pe + pH conditions. A new diffraction peak at $2\theta = 41.1°$ corresponding to goethite was found in the RE soil under low pe + pH conditions, suggesting new growth of goethite on the original minerals. The new growth of goethite might be related to the re-crystallization of poorly crystalline Fe oxides (possibly ferrihydrite) catalyzed by soluble Fe(II) under reduced conditions (Liu et al., 2005).

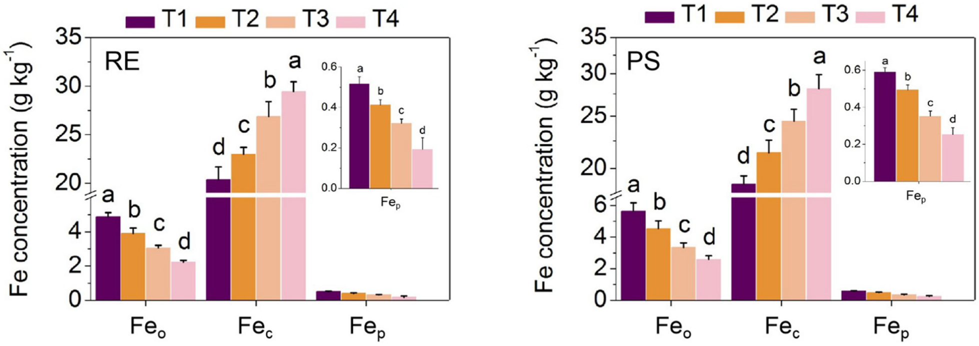

Fig. 2. Contents of crystalline Fe oxide (Fe_c), poorly-crystallized Fe (Fe_o), organically-complexed Fe (Fe_p) in RE and PS soils under various pe + pH levels. Different letters indicate significant differences in terms of different pe + pH conditions ($P < 0.05$).

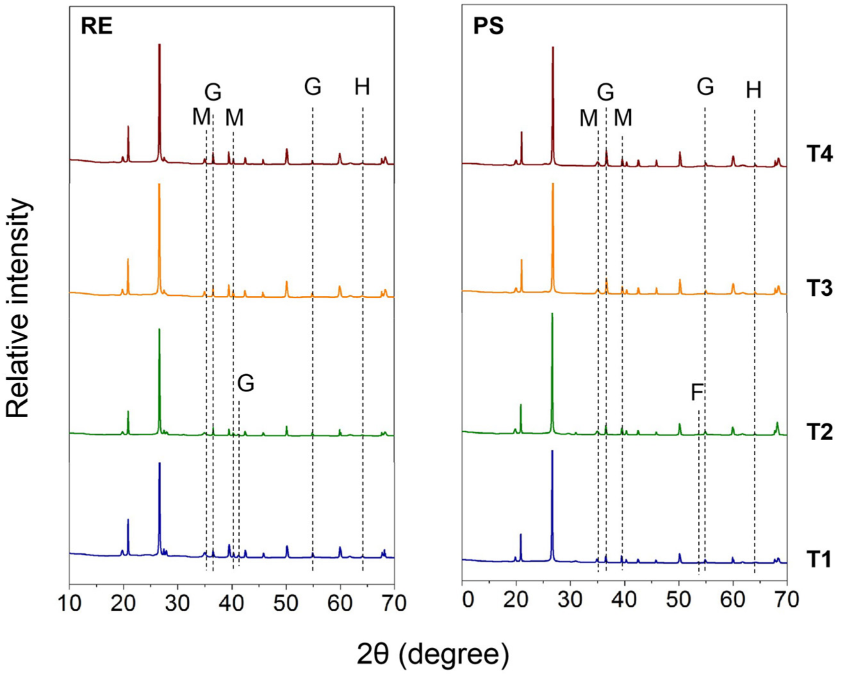

Fig. 3. X-ray diffraction patterns of Fe oxides in paddy soils under different treatments (F = 6-line ferrihydrite; G = Goethite; H = hematite; M = Magnetite).

3.2. Distribution of Fe oxide species in aggregates

The distribution of Fe oxides in different-sized soil fractions is presented in Fig. 4. Changes in soil pe + pH conditions primarily altered the concentration of Fe_t in the fractions of 0.2–2 mm and <0.002 mm, while no significant change in the fractions of 0.002–0.02-mm and 0.02–0.2-mm was observed. Fe_t concentrations decreased significantly (by 17.8%–30.6% in the 0.2–2-mm fraction and 20.7%–31.7% in the <0.002-mm fraction) under T1 and T2 treatments compared to those of the T4 treatment. Under reduction treatments (T1 and T2), Fe(III) oxides in aggregates were reduced or partly dissolved into soil solution, and then possibly adsorbed on mineral surface or entering into mineral structures. The release of Fe from aggregates resulted in Fe loss from the fractions (0.2–2-mm and <0.002-mm) originally containing more Fe. Also, soil submergence decreased the cementing effects of binding agents (iron oxides, aluminum oxides, polysaccharides, etc.) on soil aggregates formation, which promoted the disintegration of Fe-containing macro-aggregates into micro-aggregates and even the breakdown of micro-aggregates (Six et al., 2000). In this process, partial Fe oxides originally acted as the adhesives would be desorbed from aggregate surface along with the disaggregation. Thus, the Fe_t concentration in the fractions of 0.2–2-mm and <0.002-mm decreased significantly under T1 and T2 treatments. Considering the influences of aggregates disintegration and Fe(III) reduction, Fe_t content in 0.002–0.2-mm fraction may also have decreased under flooded condition. But the non-significant change in Fe_t content may be due to the translocation of Fe from fine to coarser soil aggregates or the formation of larger aggregates by the complexation of SOM with Fe-bearing fine soil particles (Huang et al., 2016).

With decreasing pe + pH value, Fe_c concentration in the fractions of 0.2–2-mm and <0.002-mm decreased by 27.4%–45.2% and 27.7%–41.3% respectively; while Fe_c concentration in 0.002–0.2-mm fraction did not change significantly. Conversely, the contents of Fe_o and Fe_p increased significantly (by 0.29–2.50-fold for Fe_o and 0.41–1.80-fold for Fe_p) with the drop in pe + pH level in the macro-aggregate and coarse micro-aggregate groups (0.002–2 mm). These results suggest that the low pe + pH condition exacerbated the reductive dissolution of Fe(III) oxides and accelerated the formation of poorly-crystallized and organically complexed Fe oxides in the four particle-size fractions. The disintegration of aggregates as well as the reduction and phase-transformation of crystalline Fe oxides under low pe + pH conditions might play critical roles in the dramatic decrease of Fe_c concentration in the macro-aggregate and fine aggregate fractions. The oxidation and hydrolysis of dissolved Fe(II) and the transformation of crystalline iron oxides into amorphous (weak crystalline) phase at low pe + pH level, promoted the accumulation of amorphous iron oxides in 0.002–2-mm fraction (Huang et al., 2016). More amorphous Fe oxides complexed with the accumulated organic matter under reduction conditions, resulting in prominent increase of Fe_p content in coarse particles (0.002–2 mm). The dissolution of Fe oxides in overlying water may have also contributed to the decrease in concentrations of Fe_c and Fe_o in the <0.002-mm aggregates at lower pe + pH conditions. Additionally, the increased Fe_o and Fe_p contents and decreased Fe_c content were observed with soil aggregate increased from micro to macro size under the T1 and T2 treatments, which may be attributed to the phase transformation of well-crystallize iron oxides into amorphous and organically-complexed forms. The gradual raised Fe_o and Fe_p contents also indicated that a low pe + pH condition may be conducive to the aggregation of small-scale soil particles due to the accumulation and complexation of amorphous Fe oxides and organic matter (Xue et al., 2019a).

3.3. Soil Cd speciation under different pe + pH conditions

The amount of Cd bound to iron/manganese oxides in soils showed a significant increase ($P < 0.05$) with the decrease of pe + pH (Fig. 5a). The concentration of OX-Cd in soils at lower pe + pH levels was 11.7%–36.6% higher than that under the T4 treatment (high pe + pH level). This indicated that a low pe + pH value favored the immobilization of Cd by iron oxides, which may be related to the obvious increase in contents of Fe_o and Fe_p at low pe + pH levels. Although the crystalline Fe oxides, such as hematite, magnetite, etc., have been reported to exhibit great ability for Cd stabilization, the rougher surfaces and larger area of amorphous iron oxides may provide more active sites for Cd adsorption compared to crystalline iron oxides (Muehe et al., 2013; Zhang

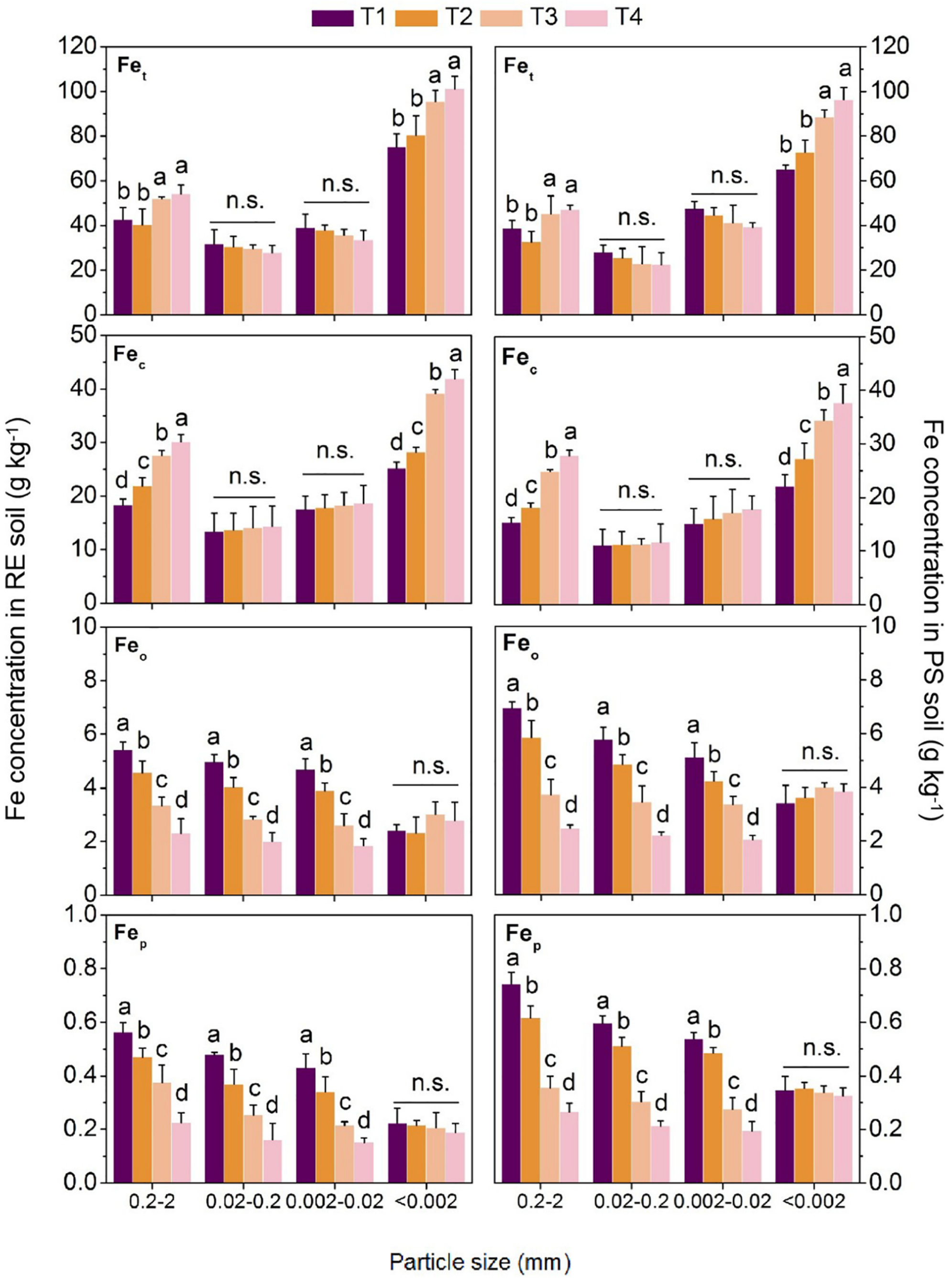

Fig. 4. The total Fe (Fe_t), crystalline Fe (Fe_c), poorly-crystallized Fe (Fe_o), and organically-complexed Fe (Fe_p) in different-sized aggregates under various pe + pH conditions. Different lowercase letters indicate significant differences among treatments for the same particle-size fraction ($P < 0.05$). Non-significant differences at $P < 0.05$ are indicated by "n.s.".

et al., 2016; Li et al., 2019). Secondly, the negative charges on Fe oxide surfaces increased due to the rise of soil pH under reducing conditions, which was also beneficial for Cd^{2+} adsorption (Zhu et al., 2018). Thirdly, the iron-sulfide complexes formed at low pe + pH levels also exhibited high adsorption capacity for Cd (Yu et al., 2016). The reaction between H_2S/HS^- and Fe(II) produced by the reductions of S and Fe under the reduced condition likely contributed to the formation of soluble FeS or solid Fe sulfides, which also promotes Cd sequestration (Li et al., 2012; Yu et al., 2016). Notably, the reductive dissolution of Fe(III) oxides under anoxic condition is coupled to the release of Cd adsorbed on iron minerals, while the soluble Fe^{2+} produced by the reduction of Fe (III) oxides can precipitate with surplus Fe(III) oxides to generate secondary iron minerals (Li et al., 2019). These newly-formed minerals with low crystallinity and abundant hydroxyl groups can re-adsorb Cd in soil solutions (Muehe et al., 2013). Furthermore, the recrystallization of metastable Fe(III) oxides, such as ferrihydrite and lepidocrocite, can also incorporate Cd into secondary minerals by metal substitution (Ishikawa et al., 2004; Yu et al., 2016). Because of all the reasons described above, it was no surprise that more Cd was present in Fe/Mn-oxide-bounded forms under the anoxic condition than compared to that in the oxygenated condition.

More research has focused on available Cd in soils in its various chemical forms due to its high mobility, bioavailability and potential toxicity. In this study, the content of available Cd in soils was represented by DTPA-extractable Cd, of which concentrations declined (by 14.1%–41.8%) with decreasing soil pe + pH and ranged from 0.619 to 0.401 mg kg^{-1} in the RE soil and from 0.569 to 0.321 mg kg^{-1} in the PS soil (Fig. 5b). This decrease in DTPA-Cd concentration at lower

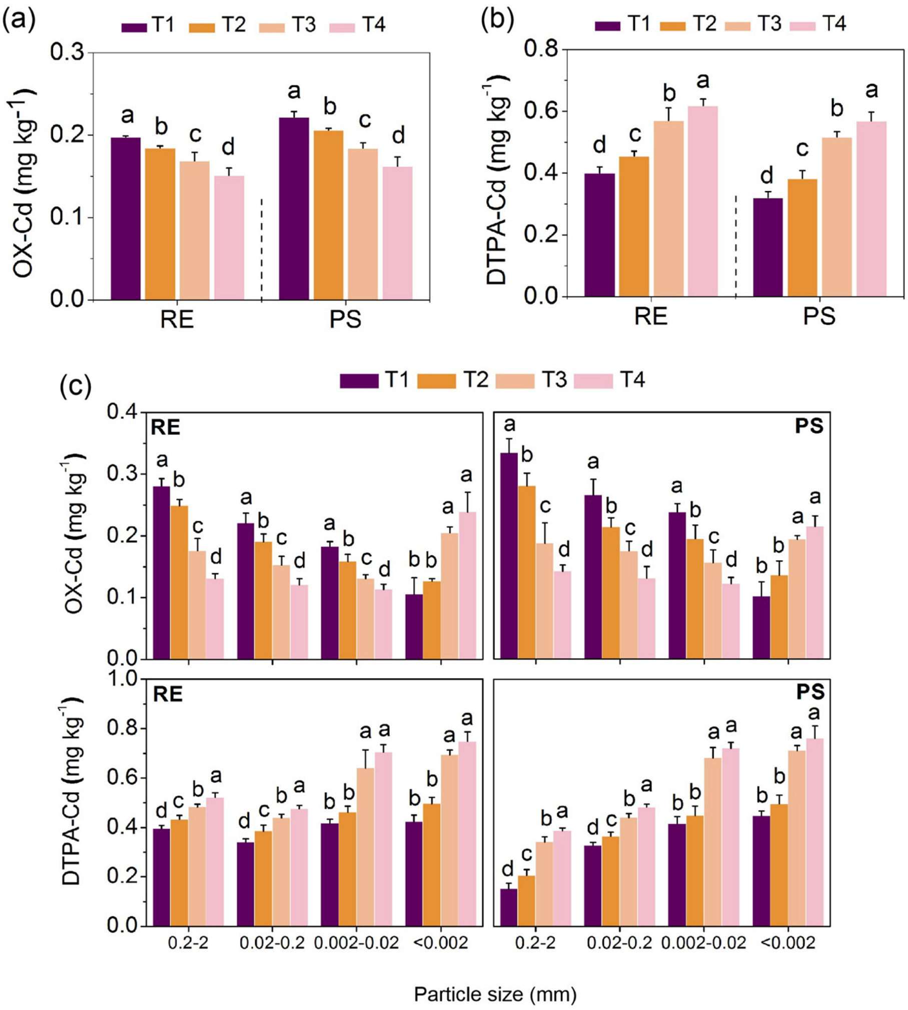

Fig. 5. Soil concentrations of Cd bound to Fe—Mn oxides (OX-Cd) (a) and DTPA-extractable Cd (DTPA-Cd) (b) and contents of OX-Cd and DTPA-Cd in different particle-size fractions (c) under various pe + pH conditions.

pe + pH level was likely due in part to more Cd being retained in iron oxides under the reducing conditions. The integration of Cd with iron oxides reduced Cd availability in soil by converting Cd from an available to unavailable form (Li et al., 2019). Meanwhile, rising soil pH under anaerobic conditions increased negative charges not only on the surfaces of iron oxides, but also on the surfaces of other soil particles which promotes their adsorption of Cd to reduce Cd mobility (Sun et al., 2007). The complexation of Cd with accumulating SOM in anoxic soils also contributed to the decline in Cd availability (data not shown). Additionally, the precipitation of Cd sulfides may occur at pe + pH values below 4.85; and Cd can also adsorb to carbonate minerals and exist as carbonates at pH levels above 5.66 (Brennan and Lindsay, 1996). Thus, the sulfides and carbonates may also have contributed to the decrease of Cd availability in our soil samples. In the present study, the complexation of Cd with sulfide minerals may have only occurred in T1-treated soils (pe + pH below 4.85). The variation in Cd-bearing carbonate minerals of the different treatments might be negligible because the change in soil pH in this study may have been insufficient to affect carbonates.

The changes in soil pe + pH conditions altered Cd speciation in various particle-size fractions (Fig. 5c). The concentration of OX-Cd in the 0.002–2-mm fraction increased significantly with declining pe + pH values, while DTPA-Cd content notably decreased at low pe + pH levels compared to contents at high pe + pH levels. The significant increases in contents of Fe_o and Fe_p in larger aggregates under reduced conditions (Fig. 4) may have contributed the binding of Cd to Fe oxides, and subsequently decreased the available Cd content in the same fractions. The dramatic decline of OX-Cd content in micro-aggregates under flooding treatments (T1 and T2) may be partly attributed to the loss of Fe due to reductive dissolution of Fe oxides, and it may also be partly associated with Cd migration from the fine particle-size fraction into coarser ones. Additionally, the OX-Cd content gradually increased with increasing aggregate size, corresponding to the DTPA-Cd content decrease, suggesting that a low pe + pH condition may favor Cd accumulating in coarser particle-size fractions in the forms of Fe-oxide-bound Cd.

Notably, both the contents of OX-Cd and DTPA-Cd in <0.002-mm fraction decreased under low pe + pH levels. The conflicting result suggested that iron oxides were not the single factor to influence Cd availability in micro-aggregate. Under reduced conditions, the complexation of Cd with organic matter and the precipitation of Cd with reduced S, as well as Cd^{2+} hydrolysis-precipitation and the enhancement of Cd adsorption by fine soil particles caused by rising pH, could together contribute to decreased Cd availability in fine aggregate. The elevation of OX-Cd content in larger-size fractions might be a crucial mechanism for the reduction of Cd availability in soils exposed to low pe + pH conditions. However, the changes of DTPA-Cd content in particle-size fractions did not absolutely correspond to that of OX-Cd content, indicating that the redistribution of Fe oxide was an important but not the sole factor affecting Cd availability in different-sized aggregates. More investigation is needed about the influence of parameters (eg. organic matter, S, pH) on Cd availability in different soil aggregates in the future research.

3.4. Correlations among soil pe + pH, Fe oxides and Cd speciation

Correlation coefficients among Fe oxides, soil pe + pH, and Cd species were calculated using the Python programming language and presented in Fig. 6. According to the coefficients, soil pe + pH was negatively correlated with the contents of Fe_o and Fe_p ($P < 0.01$), while it was positively related to Fe_c content ($P < 0.01$), further confirming that the Fe oxides crystallinity decreased with the drop of soil pe + pH value. The well-crystalline iron oxides such as hematite and goethite were reduced under low pe + pH conditions, and they may have been transformed into amorphous and organically-complexed forms (such as ferrihydrite), which was supported by the XRD results (Fig. 2). Soil pe + pH value was also closely associated with Fe_t concentration in particle-size fractions. The change in pe + pH

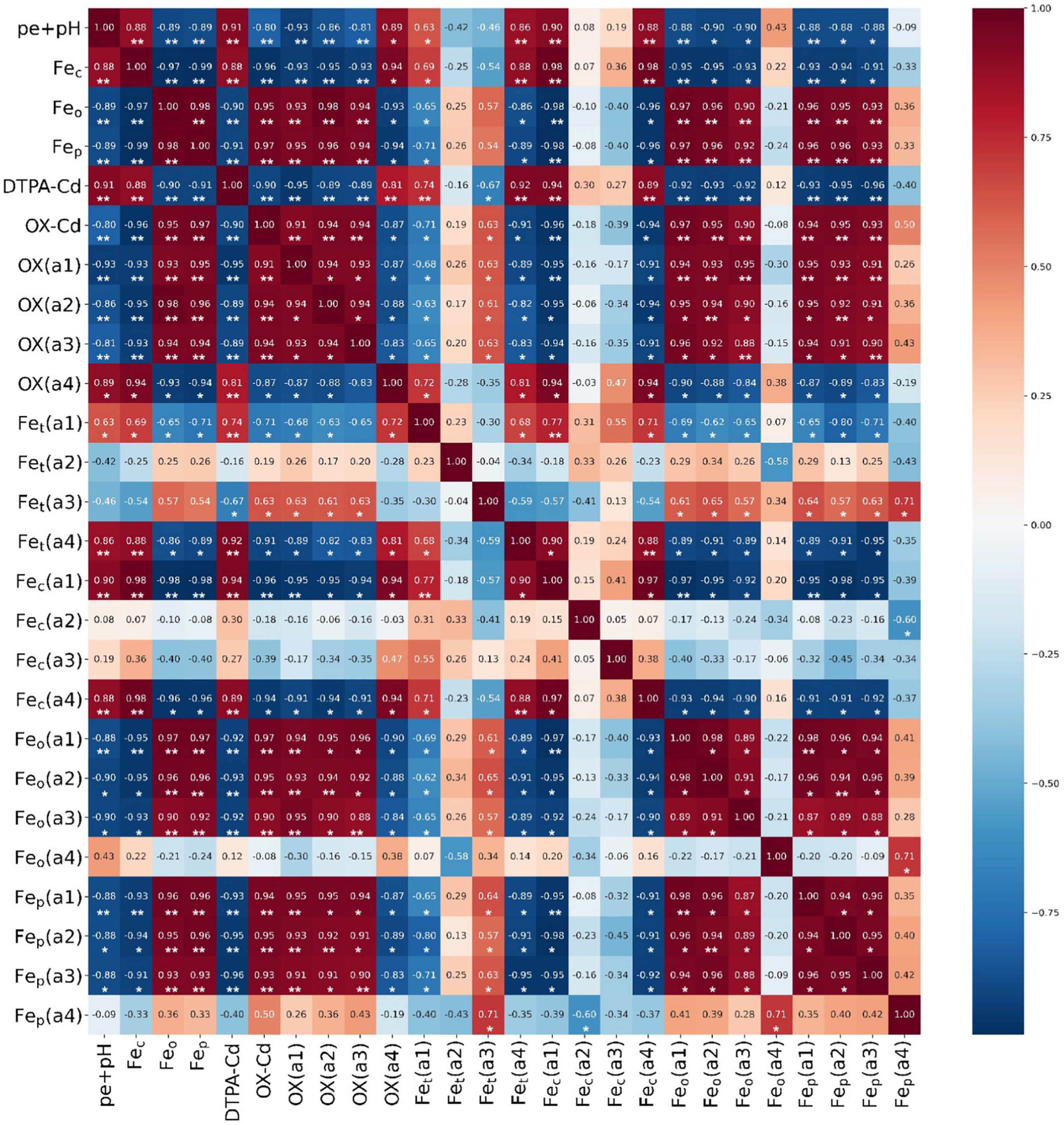

Fig. 6. Correlations among soil pe + pH, Fe oxides and Cd speciation in soil fractions. The numbers in the grid represent the correlation coefficients. Cd-DTPA and Cd-OX are the concentrations of DTPA-extractable Cd and Fe/Mn-oxide-bound Cd, respectively. OX(ai), Fe_t(ai), Fe_c(ai), Fe_o(ai), Fe_p(ai) respectively indicate the concentrations of OX-Cd, total Fe, Fe_c, Fe_o and Fe_p in different-sized aggregates. $i = 1, 2, 3$ and 4 where the numbers represent the respective particle sizes of 0.2–2 mm, 0.02–0.2 mm, 0.002–0.02 mm, and <0.002 mm. Single asterisk (*, $P < 0.05$) and double asterisk (**, $P < 0.01$) indicate statistically significant differences between values.

level primarily influenced Fe distribution in the large or smallest particle-size fraction potentially by affecting integration/disintegration of soil particles and redox behavior of Fe oxides in these fractions. Meanwhile, Fe_t concentration in the 0.2–2-mm fraction was closely related to Fe_c ($r = 0.77$, $P < 0.01$), Fe_o ($r = -0.69$, $P < 0.05$), and Fe_p ($r = -0.65$, $P < 0.05$) concentrations in the same fraction; but the Fe_t content in the <0.002-mm fraction had only significant correlation with Fe_c ($r = 0.88$, $P < 0.01$) in the same fraction. This result illustrates that the distribution of Fe in differently-sized aggregates may have principally depended on Fe_c content in different aggregates, possibly owing to the large proportion of well-crystallized Fe oxides in total Fe.

The significant and negative correlation between contents of DTPA-Cd and OX-Cd was observed, where OX-Cd content was positively associated with the amounts of Fe_o and Fe_p ($P < 0.01$). The low pe + pH condition accelerated the formation of amorphous and organically-complexed Fe oxides that have high affinity for Cd, resulting in more Fe-oxide-bound Cd and thus reducing Cd availability in paddy soils. More importantly, the amount of available Cd appeared to be mainly determined by OX-Cd concentration in coarser aggregates, because OX-Cd content in larger aggregates (0.002–2-mm) showed stronger correlation with DTPA-Cd content ($|r| > 0.89$, $P < 0.01$) than that in fine aggregates ($r = 0.81$, $P < 0.01$). The increase of OX-Cd content in coarser aggregates at low pe + pH level suggested that more Cd would be immobilized in larger aggregates in an unavailable form, and subsequently reducing Cd mobility in soil. Meanwhile, OX-Cd content was significantly and positively associated with the contents of Fe_o and Fe_p in the 0.002–2-mm fraction, suggesting the increase in OX-Cd content in larger aggregates was primarily related to more Cd bound to iron oxides due to the increase of Fe_o and Fe_p contents. Therefore, the increase in contents of Fe_o and Fe_p in coarser aggregates, caused by the transformation of crystalline Fe oxides at low pe + pH level, may result in more Cd accumulated in coarse-grained soil via sequestration by Fe oxides, ultimately reducing the amount of available Cd in paddy soil.

4. Conclusions

The decreases of pe + pH value in RE (from 11.37 to 3.42) and PS (from 11.92 to 3.98) soils caused significant decreases in the contents of Fe_c (from 33.6% to 8.60%) and increases in contents of Fe_o (from 30.3% to 119%) and Fe_p (from 39.1% to 167%). Under low pe + pH conditions, partial crystalline Fe oxides, such as hematite and goethite, were reduced, dissolved and then transformed into poorly-crystallized Fe oxides (i.e. ferrihydrite). Though some metastable Fe oxides might have converted into new goethite. The concentrations of Fe_c in the particle-size fractions of 0.2–2-mm and <0.002-mm and the contents of Fe_o and Fe_p in the 0.2–2-mm fraction were closely related to Fe distribution in differently-sized aggregates under unstable pe + pH conditions. The increases in contents of Fe_o and Fe_p in the 0.002–2-mm fractions were significantly and positively related to OX-Cd content in coarser aggregates that was mainly responsible for DTPA-Cd content in soil. In conclusion, the phase-transformation of Fe oxides driven by low pe + pH conditions increased low-crystalline and organically-complexed Fe oxides in larger aggregates, which facilitated Cd accumulation in coarser-grained soil by Fe oxide adsorption, and thus reducing Cd availability in paddy soil. This result presented the potential mechanism of pe + pH variation on Cd availability in paddy soil. Further research should be carried out in combination with agricultural production to provide a convenient method for in-situ Cd stabilization in paddy soil.

CRediT authorship contribution statement

Shanshan Li: Investigation, Data curation, Writing - original draft. **Shibao Chen:** Conceptualization, Methodology. **Meng Wang:** Conceptualization, Validation, Writing - review & editing. **Xiaoqin Lei:** Software, Validation. **Han Zheng:** Software, Validation. **Xiaoyi Sun:** Validation, Software. **Lifu Wang:** Validation, Software. **Yun Han:** Validation.

Declaration of competing interest

The authors declare that they have no known competing financial interests or personal relationships that could have appeared to influence the work reported in this paper.

Acknowledgements

This research was financially supported by the Natural Science Foundation of China [41877387] and Fundamental Research Funds for Central Non-profit Scientific Institution [1610132020025 & 1610132020027].

References

Borch, T., Kretzschmar, R., Kappler, A., Cappellen, P.V., Campbell, K., 2010. Biogeochemical redox processes and their impact on contaminant dynamics. Environ. Sci. Technol. 44 (1), 15–23.

Brennan, E.W., Lindsay, W.L., 1996. The role of pyrite in controlling metal ion activities in highly reduced soils. Geochim. Cosmochim. Ac. 60 (19), 3609–3618.

Brennan, E.W., Lindsay, W.L., 1998. Reduction and oxidation effect on the solubility and transformation of iron oxides. Soil Sci. Soc. Am. J. 62 (4), 930–937.

Fan, J.X., Wang, Y.J., Liu, C., Wang, L.H., Yang, K., Zhou, D.M., Li, W., Sparks, D.L., 2014. Effect of iron oxide reductive dissolution on the transformation and immobilization of arsenic in soils: new insights from X-ray photoelectron and X-ray absorption spectroscopy. J. Hazard. Mater. 279, 212–219.

Hanif, M., Demooy, C.J., Lindsay, W.L., 1986. The effect of alternate flooding and drying on the pH and redox of submerged rice soil. J. Agron. Crop Sci. 156, 253–259.

Huang, X.L., Jiang, H., Li, Y., Ma, Y.C., Tanga, H.Y., Ran, W., Shen, Q.R., 2016. The role of poorly crystalline iron oxides in the stability of soil aggregate-associated organic carbon in a rice-wheat cropping system. Geoderma 279, 1–10.

Huang, X.L., Tang, H.Y., Kang, W.J., Yu, G.H., Ran, W., Hong, J.P., Shen, Q.R., 2018. Redox interface-associated organo-mineral interactions: a mechanism for c sequestration under a rice-wheat cropping system. Soil Biol. Biochem. 120, 12–33.

Ishikawa, T., Minamigawa, M., Kandori, K., Nakayama, T., Tsubota, T., 2004. Influence of metal ions on the transformation of γ-FeOOH into α-FeOOH. J. Electrochem. Soc. 151 (9), 185–191.

Ji, Y.P., Luo, W.Q., Lu, G.N., Fan, C., Tao, X.Q., Ye, H., Xie, Y.Y., Shi, Z.Q., Yi, X.Y., Dang, Z., 2019. Effect of phosphate on amorphous iron mineral generation and arsenic behavior in paddy soils. Sci. Total Environ. 657, 644–656.

Jiang, J., Dai, Z., Sun, R., Zhao, Z.J., Dong, Y., Hong, Z.N., Xu, R.K., 2017. Evaluation of ferrolysis in arsenate adsorption on the paddy soil derived from an Oxisol. Chemosphere 179, 232–241.

Krause, L., Klumpp, E., Nofz, I., Missong, A., Amelunga, W., Siebers, N., 2020. Colloidal iron and organic carbon control soil aggregate formation and stability in arable luvisols. Geoderma 374, 114421–114434.

Li, Y.C., Yu, S., Strong, J., Wang, H.L., 2012. Are the biogeochemical cycles of carbon, nitrogen, sulfur, and phosphorus driven by the "FeIII-FeII redox wheel" in dynamic redox environments? J. Soils Sediments 12 (5), 683–693.

Li, X.C., Yang, Z.Z., Zhang, C., Wei, J.J., Zhang, H.Q., Li, Z.H., Ma, C., Wang, M.S., Chen, J.Q., Hu, J.W., 2019. Effects of different crystalline iron oxides on immobilization and bioavailability of Cd in contaminated sediment. Chem. Eng. J. 373, 307–317.

Liu, H., Wei, Y., Sun, Y., 2005. The formation of hematite from ferrihydrite using Fe(II) as a catalyst. J. Mol. Catal. A-Chem. 226 (1), 135–140.

Lv, J., Zhang, S., Wang, S., Luo, L., Cao, D., Christie, P., 2016. Molecular-scale investigation with ESI-FT-ICR-MS on fractionation of dissolved organic matter induced by adsorption on iron oxyhydroxides. Environ. Sci. Technol 50 (5), 2328–2336.

Muehe, E.M., Adaktylou, I.J., Obst, M., Zeitvogel, F., Behrens, S., Planer-Friedrich, B., Kraemer, U., Kappler, A., 2013. Organic carbon and reducing conditions lead to cadmium immobilization by secondary Fe mineral formation in a pH-neutral soil. Environ. Sci. Technol. 47 (23), 13430–13439.

Pan, Y.Y., Koopmans, G.F., Bonten, L.T.C., Song, J., Luo, Y.M., Temminghoff, E.J.M., Comans, R.N.J., 2014. Influence of pH on the redox chemistry of metal (hydr)oxides and organic matter in paddy soils. J. Soils Sediments 14, 1713–1726.

Qiao, J.T., Liu, T.X., Wang, X.Q., Li, F.B., Lv, Y.H., Cui, J.H., Zeng, X.D., Yuan, Y.Z., Liu, C.P., 2018. Simultaneous alleviation of cadmium and arsenic accumulation in rice by applying zero-valent iron and biochar to contaminated paddy soils. Chemosphere 195, 260–271.

Sahrawat, K.L., 2004. Organic matter accumulation in submerged soils. Adv. Agron. 81 (03), 169–201.

Six, J., Elliott, E.T., Paustian, K., 2000. Soil macroaggregate turnover and microaggregate formation: a mechanism for C sequestration under no-tillage agriculture. Soil Biol. Biochem. 32, 2099–2103.

Six, J., Bossuyt, H., Degryze, S., Denef, K., 2004. A history of research on the link between (micro) aggregates, soil biota, and soil organic matter dynamics. Soil Till. Res. 79 (1), 7–31.

Sun, L., Chen, S., Chao, L., Sun, T.H., 2007. Effects of flooding on changes in Eh, pH and speciation of cadmium and lead in contaminated soil. B. Environ. Contam. Tox. 79 (5), 514–518.

Taubner, H., Roth, B., Tippkötter, R., 2009. Determination of soil texture: comparison of the sedimentation method and the laser-diffraction analysis. J. Plant Nutr. Soil Sc. 172 (2), 161–171.

Tessier, A., Fortin, D., Belzile, N., DeVitre, R.R., Leppard, G.G., 1996. Metal sorption to diagenetic iron and manganese oxyhydroxides and associated organic matter: narrowing the gap between field and laboratory measurements. Geochem. Cosmochim. Acta. 60 (3), 387–404.

Wang, Z.H., Ma, W.H., Chen, C.C., Zhao, J.C., 2009. Light-assisted decomposition of dyes over iron-bearing soil clays in the presence of H_2O_2. J. Hazard. Mater. 168, 1246–1252.

Wang, Y., Zhang, Z.Y., Han, L.F., Sun, K., Jin, J., Yang, Y., Yan, Y., Hao, Z.N., Liu, J.F., Xing, B.S., 2019. Preferential molecular fractionation of dissolved organic matter by iron minerals with different oxidation states. Chem. Geol. 520, 69–76.

Winkler, P., Kaiser, K., Kölbl, A., Kühn, T., Schad, P., Urbanski, L., Fiedler, S., Lehndorff, E., Kalbitz, K., Utami, S.R., Cao, Z., Zhang, G., Jahn, R., Kögel-Knabner, I., 2016. Response of vertisols, andosols, and alisols to paddy management. Geoderma 261, 23–35.

Winkler, P., Kaiser, K., Thompson, A., Kalbitz, K., Fiedler, S., Jahn, R., 2018. Contrasting evolution of iron phase composition in soils exposed to redox fluctuations. Geochim. Cosmochim. Ac. 235, 89–102.

Wu, B., Amelung, W., Xing, Y., Bol, R., Berns, A.E., 2019. Iron cycling and isotope fractionation in terrestrial ecosystems. Earth-Sci. Rev. 190, 323–352.

Xue, B., Huang, L., Huang, Y., Zhou, F., Li, F., Kubar, K.A., Li, X.Q., Lu, J.W., Zhu, J., 2019a. Roles of soil organic carbon and iron oxides on aggregate formation and stability in two paddy soils. Soil Till. Res. 187, 161–171.

Xue, B., Huang, L., Huang, Y., Yin, Z., Li, X., Lu, J., 2019b. Effects of organic carbon and iron oxides on soil aggregate stability under different tillage systems in a rice–rape cropping system. Catena. 177, 1–12.

Yin, Y., Wang, L., Liang, F.H., Xi, F.M., Pei, Z.J., Du, L.Y., 2016. Soil aggregate stability and iron and aluminium oxide contents under different fertiliser treatments in a long-term solar greenhouse experiment. Pedosphere 26 (5), 760–767.

Yu, H.Y., Li, F.B., Liu, C.S., Huang, W., Liu, T.X., Yu, W.M., 2016. Chapter five-iron redox cycling coupled to transformation and immobilization of heavy metals: implications for paddy rice safety in the red soil of South China. Adv. Agron. 137, 279–317.

Zhang, P., Zheng, J., Pan, G., Zhang, X., Li, L., Rolf, T., 2007. Changes in microbial community structure and function within particle size fractions of a paddy soil under different long-term fertilization treatments from the Tai Lake region, China. Colloid Surface B 58 (2), 264–270.

Zhang, C., Yu, Z.G., Zeng, G.M., Jiang, M., Yang, Z.Z., Cui, F., Zhu, M.Y., Shen, L.Q., Hu, L., 2014. Effects of sediment geochemical properties on heavy metal bioavailability. Environ. Int. 73 (4), 270–281.

Zhang, C., Yu, Z., Zeng, G., Huang, B., Dong, H., Huang, J., Yang, Z., Wei, J., Hu, L., Zhang, Q., 2016. Phase transformation of crystalline iron oxides and their adsorption abilities for Pb and Cd. Chem. Eng. J. 284, 247–259.

Zhao, J.S., Chen, S., Hu, R.G., Li, Y.Y., 2017. Aggregate stability and size distribution of red soils under different land uses integrally regulated by soil organic matter, and iron and aluminum oxides. Soil Till. Res. 167, 73–79.

Zheng, H., Wang, M., Chen, S., Li, S., Lei, X., 2019. Sulfur application modifies cadmium availability and transfer in the soil-rice system under unstable pe + pH conditions. Ecotox. Environ. Safe. 184, 109641–109648.

Zhu, B.J., Liao, Q.L., Zhao, X.P., Gu, X.Y., Gu, C., 2018. A multi-surface model to predict Cd phytoavailability to wheat (Triticum aestivum L). Sci. Total Environ. 630, 1374–1380.